Vibration Energy Harvesting for LPWAN Connected Devices

Hugo Cunha
Instituto Superior Técnico
Lisbon, Portugal
hugo.cunha@tecnico.ulisboa.pt

***Abstract*— Vibration energy harvesting has been, in recent years, the recurring object of a variety of research efforts aimed toward providing an autonomous solution to the power supply of small-scale electronic devices. Energy harvesting is the process by which energy is derived from external sources captured, and stored for small, wireless autonomous devices. Vibration sources provide energy that can be harvested to charge wireless sensors or produce electricity. This thesis presents a brief explanation of the theory behind the phenomenon of harvesting and some of the transducers used for this purpose. It clarifies how energy is obtained from vibration using transducers with three different physical principles, through a piezoelectric material, a variation in capacitance (electrostatic), and a magnet and a coil (electromagnetic). Also, it includes some examples of electromagnetic transduction devices and its operation system, emphasizing the magnetic levitation vibration harvesting transducer type. The magnetic levitation vibration energy harvesting transducer is the basis of this thesis; its structure and characteristics are presented in the beginning of this document. A transducer based on magnetic levitation is also elaborated, and the procedure used in its construction is explained. A characterization setup was developed to allow the analysis of the operation and behaviour of the transducer, when applied to different sources of vibration. The instrumentation used in the characterization setup is presented and, thanks to that instrumentation, it is possible to show the power generated by the transducer both when a sinusoidal wave is applied to the vibration generator and when an arbitrary wave that originates a simulation of real sources is applied**

.Keywords— Energy Harvesting, Vibration Energy, Electromagnetic Transducer, Magnetic Levitation Energy Harvesting Transducer.

I. INTRODUCTION

Internet of things (IoT) is defined by objects that are capable to transmit data over the internet or other networks and be programmed for certain applications. IoT devices are pieces of hardware, such as sensors, actuators, gadgets, appliances, or machines. These devices need batteries as power supplies, but batteries can be expensive, have great operational cost (once they need to be charged or exchanged), and are not environmentally friendly. Energy can be harvested from a wide variety of sources and an alternative to batteries is power the devices with the use of energy sources presented in environment like solar energy, thermal energy, wind energy, vibration energy, amongst others.

Currently, it is increasingly necessary to recover all the energy possible, both ecologically and economically. Vibration is an example of an energy source that is very unused, but with great potential. Handy and abundant vibration sources are not being used to generate energy, such as railway lines, human and animal movements, and all systems powered by engines, such as cars.

Energy harvesting is the process by which energy is derived from external sources, captured and stored for small, wireless autonomous devices. Vibrations present in the environment can provide energy that can be harvested to charge wireless sensors or produce electricity. There are already devices on the market that can generate energy from vibration, however they are still very expensive and little used.

This thesis aims to develop an induction-based energy harvesting transducer and its characterization understanding what instrumentation is needed to characterize it and measuring the power it can generate.

II. STATE OF THE ART

A. Energy Harvesting

Obtain large-scale harvested energy is possible through sources like wind or solar. However, to power a LPWAN device, small-scale energy harvesters working from radio waves, temperature differences, or mechanical vibrations may answer enough. So, small-scale sources such as radio waves, temperature differences, or mechanical vibrations are the possible solution for the final goal.

The process to harvest energy through temperature differences is based on the Seebeck effect, which consists on the generation of an electric potential difference between two conductors or semiconductors of different materials, having these different temperatures [1].

Energy also can be obtained through stray radio frequency and an antenna. There are two approaches, broadband and narrowband. The broadband approach can harvest more significant energy because it uses a large part of the frequency spectrum compared with the narrowband approach that uses only a small part of the frequency spectrum [2].

Mechanical vibrations can be converted to electrical energy through a transducer. The transduction mechanism can be electrostatic, through a variation at a capacitance; piezoelectric, through a piezoelectric property which is when mechanical forces applied to specific materials result in an

output voltage; and finally, electromagnetic that uses electromagnetic induction to produce energy.

B. Piezoelectric Transduction

A transducer is a device used to convert energy from one nature form to another. To occur transduction, the form of energy has to change. In the case of piezoelectric transduction, the energy conversion can be from mechanical energy to electrical energy, or vice versa.

The piezoelectric transducer, represented in Figure 1, is a type of transducer that converts the electrical charges produced in some materials with a specific characteristic into energy. The material has the characteristic of when is subject to pressure or stress, generates a voltage. Typically, the vibration of the environment around the energy collection device is the cause of mechanical stress. The word "piezoelectric" is defined literally by electricity caused by pressure or stress. This phenomenon is called direct piezoelectric effect [3].

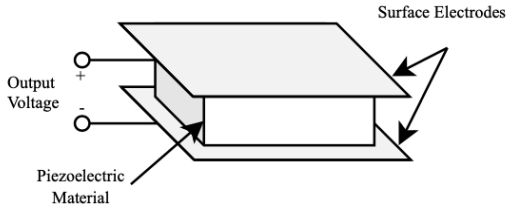

Figure 1- Piezoelectric schematic.

1) Piezoelectric Harvester Design

To obtain the best electromechanical coupling, many types of transducers were developed. However, the structures that use a free cantilever beam are the most usual. The cantilever beam structure consists of three main parts, the cantilever beam, the seismic mass, and piezoelectric layers as can be seen in the Figure 2 [4].

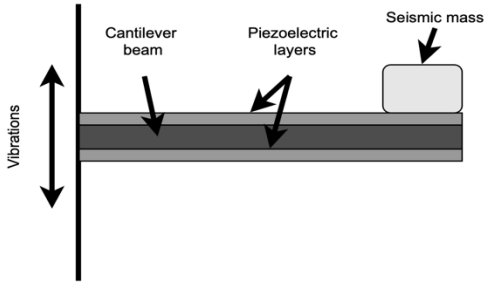

Figure 2- Basic cantilever beam harvester structure.

The cantilever beam is the basis of the structure and serves to amplify the relative displacement of the seismic mass to the vibration source's displacement amplitude. The seismic mass originates a higher output power because it increases the mechanical stress applied to the piezoelectric material. Finally, the active part of the structure, the piezoelectric layers that are used to convert mechanical vibrations into electrical energy.

With the goal of increase the movement of the seismic mass and consecutively increase the impact on the piezo material and harvest more energy, magnets are added to the circuit [5]. As can be seen in figure 3, the unique difference is the addition of four permanent magnets.

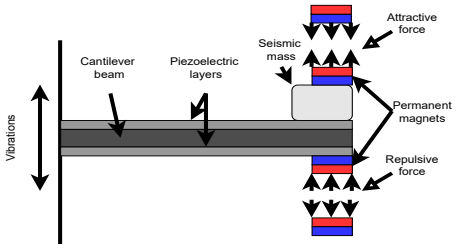

Figure 3- Basic cantilever beam harvester structure.

C. Electrostatic Transduction

A capacitance structure made of two parallel metal plates separated by air, vacuum, or dielectric materials, also named capacitor, is responsible for the electrostatic transduction. A capacitance variation is generated when a relative movement between the two plates occurs. Electric charges appear on the plates when there is a capacitance variation. There are two categories of this devices, electret free and electret based.

1) Electret free

Electret free electrostatic converters are passive structures that require an energy cycle to convert mechanical energy into electrical energy.

The charge-constrained cycle (Figure 4) is the most straightforward to implement on electrostatic devices Only when capacitance reaches max value C_{max} (1) the cycle starts. The capacitor store an electric charge Q_{ctn} provided by an external source U_{min}. The device is then let in an open circuit (2), and when the structure moves mechanically to a position where its capacitance is minimal (3), the capacitance C decreases and the voltage across the capacitor U increases because Q_{ctn} was kept constrained. Electric charges are removed from the structure (4) when the capacitance reaches its minimum (C_{min}) or when the voltage reaches its maximum (U_{max}) [6].

The quantity of energy harvested at each cycle can be obtained through the following formula

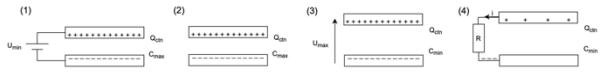

Figure 4- Charge-constrained cycle.

$$E = \frac{1}{2} Q_{ctn}^2 \left(\frac{1}{C_{min}} - \frac{1}{C_{max}} \right) \quad (1)$$

As the charge-constrained cycle, the voltage-constrained cycle (Figure 5) starts when the electrostatic converter's capacitance is maximal. The capacitor is polarized using a constant external power supply (1). The constant and external voltage applied, originate capacitance decreases, and the capacitor's charge increases, generating a current that is scavenged and stored (2). When the capacitance reaches its

minimum value, the charge Q still presents in the capacitor is ultimately collected and stored (3).

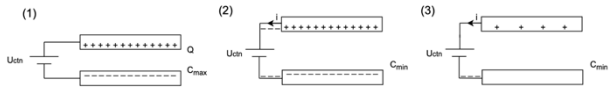

Figure 5- Voltage-constrained cycle.

The total amount of energy harvested at each cycle can be obtained through the following formula

$$E = U_{ctn}^2(C_{max} - C_{min}). \quad (2)$$

2) Electret based

Electret-based electrostatic converters are very similar to electret-free electrostatic converters. The electret layers added on one or two plates of the variable capacitor, polarizing it, are the main difference and make converse do not need any extern power supply.

The electret-based conversion device does not need any initial electrical energy to work. A structure deformation induces an output voltage directly, just like a piezoelectric material. The electret induces charges on electrode and counter-electrode, so the electret charges are distributed between electrode and counter-electrode. Therefore, the sum of Q1 (total amount of charges on the electrode) and Q2 (total amount of charges on the counter-electrode) is equal to the electret's charge, Qi, (Qi=Q1+Q2).

A relative movement between the counter-electrode and the electret and electrode induces a change in the capacitor geometry. When the counter-electrode moves away from the electret, the air gap changes, changing the electret's influence on the counter-electrode. It causes a reorganization of charges through load R (Figure 6) among the electrode and the counter-electrode. The relative movement between the counter-electrode and the electret and the electrode results in a current circulation through the resistance, R, and one part of the mechanical energy (relative movement) can be turned into electricity [6].

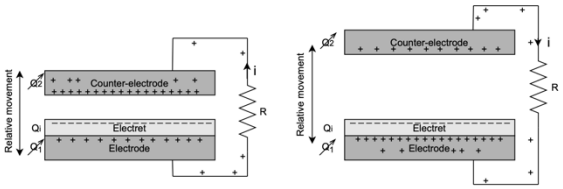

Figure 6- Charge circulation of electret-based electrostatic conversion.

If at the terminals of the electret-based converter were a simple load resistance, the differential equation that characterizes the converter is

$$\frac{dQ_2}{dt} = \frac{V_S}{R} - \frac{Q_2}{C(t)R}. \quad (3)$$

D. Eletromagnetic Tansduction

Electromagnetic induction is the basis of electromagnetic transduction. Electromagnetic induction happens when a conductor is placed close to a magnetic field, and the magnetic field continues to vary, or the magnetic field is stationary, and the conductor moves over the magnetic field. It is This phenomenon happens due to Faraday's law. This law relates the magnetic flux variation rate through a conductor (coil) to the electromotive force magnitude induced in that conductor [7].

Any electromagnetic transducer structure must have three items, a magnet, a coil, and a vibration source to make the magnet move. The magnet generates the magnetic field and the coil that is a conductor and finally, the most crucial part, the source that makes the magnet move. The relative movement between the coil and the magnet originate a magnetic flux variation that give rise to magnetic induction.

The spring has an essential function of absorbing external vibrations and consecutively make the magnet move in regard to the coil. As shown in Figure 7, the magnet oscillates inside the coil according to the vibration source, inducing an electromotive force [8].

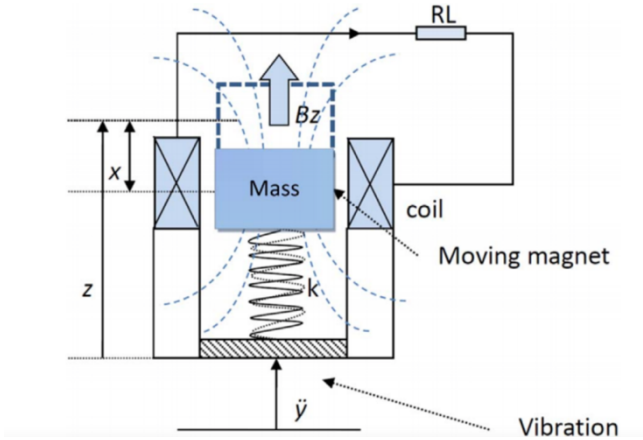

Figure 7- Electromagnetic vibration transducer model.

1) One-Magnet Spring_based Electromagnetic Energy Harvesting

The one-magnet spring-based Electromagnetic Energy Harvester is a design that brings better results. As shown in the Figure 8, it is constituted by a non-metallic cylindrical structure that contains one magnet and two helical springs, one connected to the top of the magnet and top of the structure and the other connected to the bottom of the magnet and bottom of the structure. To be able to harvest the energy, there is also a coil around the magnet outside the structure.

Due to an external vibration source, the helical springs absorb the vibration, causing the magnet to move through the coil and consequently alter its magnetic flux, inducing a voltage in the coil [9].

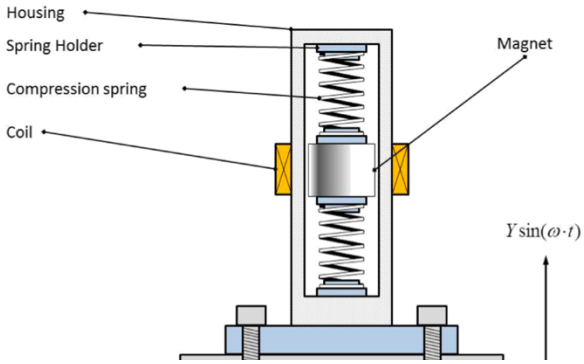

Figure 8- One-Magnet Spring-Based Electromagnetic Energy Harvester design [9].

The top spring eliminates the gravitational force effect acting on the magnet. Compared to the previous example, the oscillations of this topology have less damping effect. However, this vibration energy harvester device has a significant disadvantage. The springs bring to the harvester device the buckling effect resulting from the sudden change in the spring's shape under a load (deformation). It makes the springs to consuming part of vibrational energy and its damage. This lead to a system performance degradation over time.

2) Flux-Guided Magnet Electromagnetic Energy Harvester

Flux-guided Magnet Stacks Electromagnetic Energy Harvester is based, as presented in Figure 9, on a non-metallic cylindrical structure that contains two generators and a free inertial mass, responsible for inducing current at the generators. There is a generator located at each side of the apparatus. Each generator is composed of a helical spring connecting the top or bottom of the structure to the magnet, and each generator has a coil around the magnet outside the structure.

The freely movable inertial mass is a non-magnetic metal ball responsible for making the magnets move, generating electrical energy. It needs a specific motion source to the inertial mass hit at the magnet with the maximum inertial energy to obtain the maximum energy harvesting.

The impact of the inertial mass results in springs vibrations, and generators transfer the mechanical energy into electrical energy under electromagnetic induction [10].

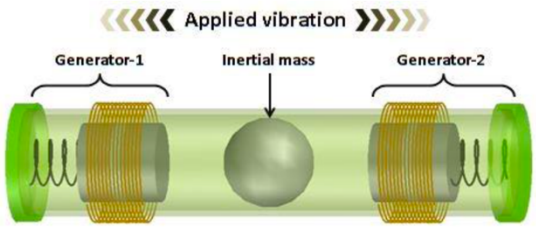

Figure 9- Flux-Guided Magnet Stacks Electromagnetic Energy Harvester design [10].

The principal handicap of this electromagnetic energy harvester is that the motion's source must be efficient and specific (arrows direction). Only like that, the mechanical force applied to the magnet will be the maximum to obtain the maximum electrical energy. The inertial mass impact on the magnets will be damaging the mass and the magnets over time and as the one-magnet spring-based electromagnetic energy harvester presented above, the use of springs has the disadvantage of the buckling effect's appearance.

3) Magnetic Levitation Vibration Energy Harvesting Transducer

Considering the disadvantages that the springs bring to the electromagnetic energy harvesters, a device that avoided its use was proposed. It is also essential to make the vibration sources nonspecific could be implemented the harvester in several situations and locals.

Maglev electromagnetic harvester is based on the levitation phenomenon. As can be seen in the Figure 10, the magnetic levitation harvester consists of two magnets, one on the top and the other on the bottom, mounted inside a cylindrical non-magnetic tube. The fixed magnets are levitating the third magnet because each magnet pair with magnetic poles oriented to repel causes the levitation force. The coil is situated outside the tube, around the levitation magnet. Air compressively attenuates the levitation magnet's movement, so holes were made on the tube to solve this situation. External vibrations on the tube originate oscillations on the moving magnet and magnetic flux changes [11].

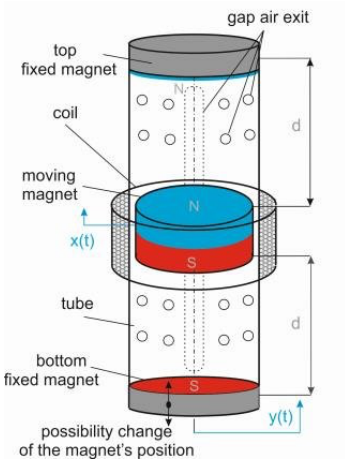

Figure 10- Maglev Electromagnetic Energy Harvester design [12].

III. CHARACTERIZACTION SETUP

One of the objectives of this thesis was to analyse the transducer and its behaviour to optimize it. In the absence of a setup capable of analysing it, the priority was to build a setup that allows the control and careful analysis of the transducer.

As observed in Figure 11, the characterization setup was composed of an instrumentation block, whose architecture will be explained below. The instrumentation block provided the vibration stimulus to the transducer and acquired the EMF generated by the transducer. Furthermore, the instrumentation block interacted with a computer with a LabVIEW software responsible for processing and controlling data received and sent.

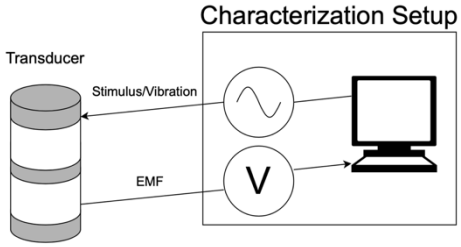

Figure 11- Characterization setup interaction the transducer.

A. Architecture

The instrumentation architecture block was designed to meet the processing and control needs required to achieve the proposed objectives. The architecture is composed of a vibration generator 2185.00, a TG1010A Programmable 10MHz Direct digital synthesizer (DDS) function generator, a audio amplifier, a USB-6009 acquisition board (DAQ), a ADXL357 accelerometer, and a programmable resistance substitute. The characterization setup can be seen in the Figure 12.

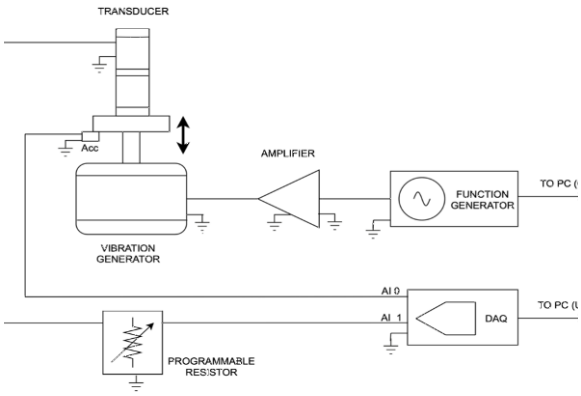

Figure 12- Characterization setup.

B. Vibration Generator and Transducer Coupling Mechanism.

To test the transducer, it was essential to use a source of vibration. So, it was used the vibration generator 2185.00 that can be seen in the Figure 13 for being a more practical option that would allow testing the transducer in a laboratory environment.

Figure 13- Vibration generator 2185.00.

Once with the chosen vibration source, it was needed to couple the transducer to the vibration generator. Since the tap centre with the banana is the only part of the transducer that vibrates, the transducer would have to be attached there, so the solution found was to design and produce parts in a 3D printer to solve the problem found. First, the base part that fit the banana and then an intermediate piece where the transducer was connected that fits the base part, as shown in Figure 14.

Figure 14- Transducer coupling mechanism.

C. Signal Generator

The operation of a vibration generator is dependent on a signal imposed on its terminal inputs so it was introduced a function generator into the system, so the Programmable 10 MHz DDS Function Generator TG1010A was used, which was available in the laboratory. This function generator can generate waves programmatically through the GPIB protocol. However, the wave produced in the function generator has a very limited current capability, insufficient to make the vibration generator vibrate, so it was necessary to amplify it. So, an audio amplifier was needed to bring to the system. By requirement of the audio amplifier Audio M033N which was introduced, it was also necessary to bring to the system a voltage source.

D. Data Aquisition

With the transducer working, it was necessary to analyse the data coming from it. To analyse the vibration coming from the vibration generator for any imposed wave was used a ADXL357 accelerometer installed on the coupling mechanism. To analyse the influence of the load resistance at the transducer terminals it was utilized a programmable resistance substitute and to acquire and access this both signals it was a USB-6009 DAQ.

E. Processing and control software

In the project planning, the need to have a component for processing and controlling the system devices arose. This was necessary for testing and improving the transducer. Considering the devices used and their purpose, the most practical and most accessible option to implement the processing and controlling component is the LabView program from the National Instruments (NI) company because it is enabled with native GPIB interface libraries and DAQ support, beside all the signal processing functionalities.

The software development evolved as the devices were introduced into the system and had two versions, an initial version to characterize the transducer, and the second to test the transducer at authentic sources of vibration.

1) Transducer Characterization

The first version to characterize the transducer test the operation of all devices with a sinusoidal, square, or triangular periodic wave and the second version where the waves that are imposed on the vibration generator simulate authentic vibration sources.

In this part is effectuated a frequency and load resistance value sweep with a selected wave imposed to the vibration

generator and showed the transducer transfer function, the vibration acceleration and the electromotive force and the power generated resulting the impulse imposed.

2) Evaluation of Emulated Vibration Sources

The second version of the program emerged from this need, testing the transducer on known and authentic vibration sources.

For the system to simulate the characteristic vibration of a specific source of concrete vibration, it was necessary to apply a wave to the system input that gave rise to that same vibration source. The objective would be to find which wave apply to the input system so that the vibration generator simulates the characteristic vibration of these vibration sources after the influence of the system.

The program consists of five tabs. The first that consists of the model's characterisation was elaborated to know the influence of the system on a signal that passes through it. The second tab is responsible for selecting the vibration source to simulate in the vibration generator among those available. The third tab is responsible to program in the function generator the wave which will generate the desired vibration in the vibration generator and the fourth for improve the trustworthiness of the vibration in the vibration generator through a iteration process. And the fifth for presented the result of the simulated source like the EMF and the power generated with a load resistance value sweep.

IV. TRANDUCER DESIGN

The elaborated transducer followed the basis of the Magnetic Levitation Vibration Energy Harvesting type but with some modifications. The top magnets are fixed in the Magnetic Levitation Vibration Energy Harvesting transducer, which means the distance between the two top magnets is always the same. In the elaborated transducer, the distance between magnets can be adjusted to optimize the transducer and obtain more energy with the same vibration source. The dimensioning of the internal cylinder of the transducer was not exactly the same diameter as the magnet, it was a little wider due to difficult mechanical conditions in its dimensioning. Then, the transducer could not be designed to hold only one levitation magnet, because the inner cylinder was a little wide, and the magnet in the centre turned, due to the attraction and repulsion force from the top magnets. It was then necessary to increase the number of magnets in the levitation, which could be done with two or three central magnets. So, the transducer elaborated consists of a coil with 200 windings, five or four magnets with 15mm in diameter, and 3mm in height with 860-995 kA/m of magnetization that they are inside a polycarbonate cylinder, two 3D printed parts, and two screws.

These parts are attached to the transducer cylinder with hot glue, which allows them to be easily removed to test the transducer with two or three central magnets.

Each of the two top magnets is connected to a screw, with hot glue, that can modify its position. This capability can manipulate the central magnet's position regarding the coil due to the phenomenon of levitation and the distance of the top magnets between them. This adjustment is possible because the printed tops are designed for this purpose. The final result after assembly is shown in figure 15.

Figure 15- Transducer all assembled.

V. RESULTS

This chapter will present the transducers analysis results based on both programs elaborated, one to characterize the transducer and the other to test the transducer in authentic sources.

A. Transducer Characterization Results

The first results come from the first version of the program, where a sine wave of 2V peak-to-peak amplitude is selected with the frequency varying between 1 and 100 Hz, linearly with a step of 1 Hz. Figure 16 shows the value of the vibration acceleration caused by the selected wave and applied to the stimulation chain.

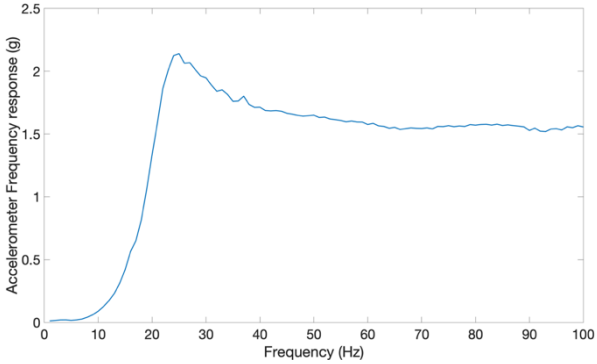

Figure 16- Accelerometer response by the selected signal.

Then, the amount of power that the transducers can generate is analysed by varying the distance between the top magnets, making a frequency and load resistance sweep. The frequency sweep is linear between 10 and 100 Hz with a 1 Hz step, and the load resistance sweep is logarithmic that vary between 1 ohm and 10K ohm in 20 points.

The analysis started by testing the generated power when the transducer had three central magnets centred with the coil and varying the distance between the top magnets and then the same test but with two central magnets. Starting with the top magnets at a distance of 6 cm, which is as far apart as possible due to the transducer characteristics, and ending at 4

cm, which is as close as possible also due to the transducer characteristics with a step of 0,5 cm.

After analysing the transducer with three and two centre magnets is presented in the Figure 17 the generated power by each distance between top magnets in both cases.

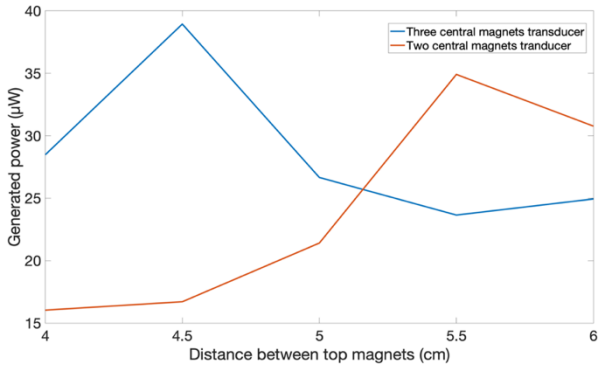

Figure 17- Maximum power generated at each distance.

It is concluded by observing the graph that there is an optimal point where the transducer can generate more energy in each case. In the case that it had three central magnets, the optimal distance was 4.5 cm between the top magnets, and in the case that the transducer had two central magnets, the ideal distance was 5.5 cm between the magnets of the tops. This difference happened because the weight of the central magnets was obviously different, which requires different intensities of the repulsion force that allows the levitation at each case.

When the transducer had three central magnets, the negative influence of the distance between the top magnets was very evident. This happened because the repulsion force between the top magnets and the central magnets was very small, originating very large oscillations by the central magnets regarding the coil, thus leaving the range of the coil and generating less energy.

On the other hand, it was very evident in the transducer when it had two central magnets the negative influence of the excessive approximation between the top magnets and the center magnets. It happens because the repulsive force between the top magnets and the center magnets was so great that it did not allow the central magnets to respond to the vibration stimulation by moving because they were stuck by the repulsive force acting on it thanks to the proximity of the top magnets.

Regarding the energy that the transducer could generate with two or three central magnets at the distances between top magnets tested, when the central magnets were centered with the coil the transducers had identical results at ideal distances.

Next, the results of the central magnets position variation relative to the coil in the transducer with two and three central magnets were compared. When the transducer had three central magnets, the displacements tested were when the central magnets go down and up 1.5 mm and 3 mm regarding to the center, and when the transducer had two central magnets, the displacements tested were only when the central magnets go down and up 1.5 mm regarding to the center. The maximum power generated at each displacement for both cases can be observed in Figure 18 and 19.

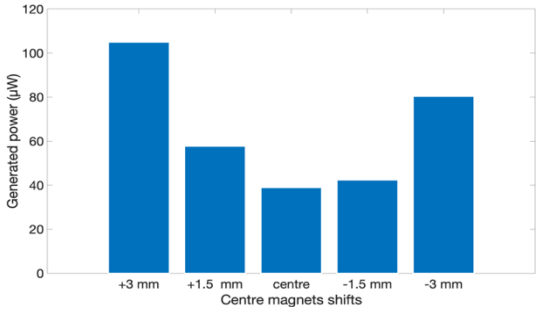

Figure 18- Maximum generated power at each displacement with three central magnets.

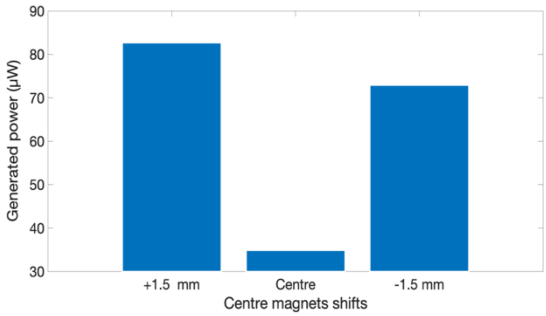

Figure 19- Maximum generated power at each displacement with two central magnets.

As the Figures 18 and 19 shows, the lowest power values were recorded when the central magnets were aligned with the coil, and the highest values when the center of the central magnets was moved so that the extremities magnets, the top or bottom, line up with the coil. This phenomenon happens because when the magnets were together, due to the attractive force between equal poles, this set worked as just one magnet. Therefore, it only presented a significant magnetic field perpendicular component gradient to the coil at the extremities.

The coil had 3 mm of height, exactly the same as each centre magnet height, which indicates that when the centre magnets moved 3mm down or up on the three centre magnets transducer, the coil became aligned with one of the extremities magnet, which was precisely where the component perpendicular to the coil of the magnetic field was strongest. This fact explains that, it is in these position that the transducer achieves the highest power results. The transducer with two center magnets had the same behaviour, it also had the highest power values when aligning the end magnets with the coil.

It was also easier to stabilize the three central magnets in the ideal position because it brought better results. While with two central magnets, the collected power was a bit lower, indicating a less successful stabilization.

The knowledge of the transducer behaviour was essential as it allows to conclude the distance between top magnets and in which position relative to the coil the central magnets should be to obtain an optimized power result. After this learning, the two central magnets transducer will be tested in real sources emulated by the vibration generator.

B. Evaluation of Emulated Vibration Sources Results

These results were achieved through the second part version of the program, responsible for testing the transducer on real vibration sources simulating them in the vibration generator. The vibration sources chosen to emulate in the vibration generator were the movement during walking of the lower leg, the water pump motor, and the car's engine.

The first source to simulate was the lower leg movement when walking, whose results can be seen in Figures 20 and 21. Figure 20 shows the optimization process at each iteration and the final signal measured by the accelerometer. Figure 21 shows the differences between the measured signal and the target signal spectrum and the electromotive force that the transducer can generate from the simulated source.

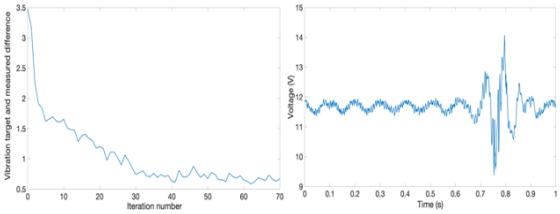

Figure 20- Optimization process and resulting signal.

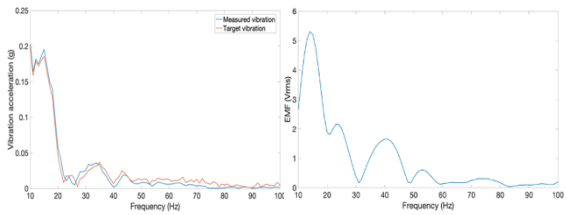

Figure 21- Measured and target vibration and EFM resulted.

As shown in Figure 20, the optimisation process was demanding. It took about 40 iterations to present a reliable result of the simulated source, reaching the final signal, also visible in Figure 20. In Figure 21, a comparison between the target signal and the signal that the accelerometer measures after the optimisation process is visible. The optimisation process achieved a good approximation, so the transducer tested on the chosen source managed to generate a maximum EMF of 5,2 Vrms, also visible in Figure 21.

Another source simulated in the vibration generator was the car engine, whose results of this simulation can be evaluated in Figures 22 and 23. In Figure 22, the optimization process at each iteration and the final signal measured by the accelerometer that measures the vibration generator vibration. And in Figure 23, the overlapped graphs of target and measured vibration together with the electromotive force generated in this simulated source.

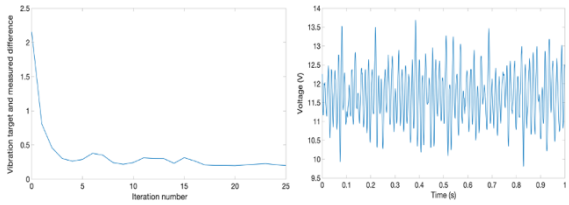

Figure 22- Optimization process and resulting signal.

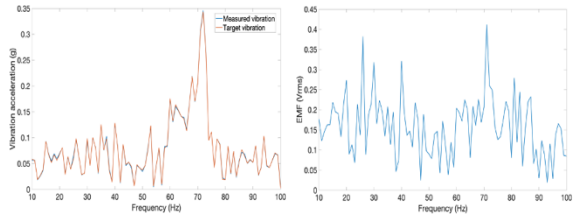

Figure 23- Measured and target vibration and EFM resulted.

The optimization process of this source was easier than the previous one, as it is visible in Figure 22, in the fourth iteration, the obtained signal was already very close to the final signal. This signal is also visible in Figure 22. In Figure 23, it is visible that the process of optimization was successful because the differences between the target and acquired signal are minimal, thus making a good replication of the vibration source to be simulated. Also, in Figure 23, it is possible to consult the EMF that the transducer could generate applied to this simulated source. It was possible to reach maximum EMF values in the order of 0,042 Vrms, values higher than those reached with the previous simulated source.

The last tested source was the water pump motor, which results are shown in the same way as the sources presented above. Results are present in Figures 24 and 25. Figure 24 shows the optimization process at each iteration and the final signal acquired by the accelerometer that measures the vibration of the vibration generator. Figure 25 shows the overlapped graphs of target and measured vibration to compare them and see if the optimization process was successful and the electromotive force that the transducer can generate applied to this source.

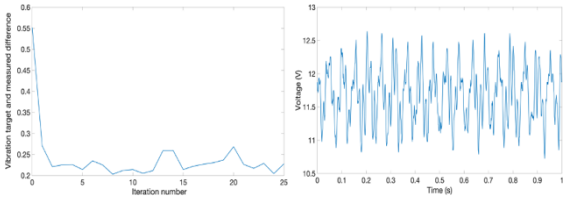

Figure 24- Optimization process and resulting signal.

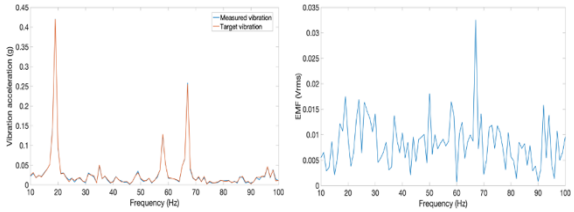

Figure 25- Measured and target vibration and EFM resulted.

The optimization process visible in Figure 24, similarly to the previous source, quickly converged to the result obtained at the end of the optimization that originated the signal, also visible in Figure 24. The objective of simulating the source in the vibration generator was successful because as shown in Figure 25, the vibration signal done by the vibration generator was very similar to the target signal. It is also visible in Figure 25 the EMF that the transducer was capable of generate when applied to the simulated vibration source. The EMF that the transducer can generate happens with a frequency of 68 Hz, and it is about 0.034 Vrms.

The results presented show that the objective of this part of the program was successfully completed, since it was possible to simulate the desired sources accurately and also to test the transducer on them. The key factor that led this test to success was the optimization tab, since only the result of the "wave programming" tab did not respond to the initial challenge of an authentic simulation.

After presenting the simulation characteristics of each of the analysed sources, it was also determined the power that each source would be able to generate, varying the load resistance at the transducer terminals. A linear sweep of the load resistance value was performed in all cases to analyse the influence of that at the transducer terminals. The results of this test can be seen in Figure 26.

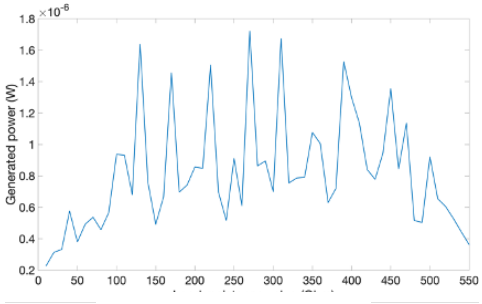

a) Lower leg.

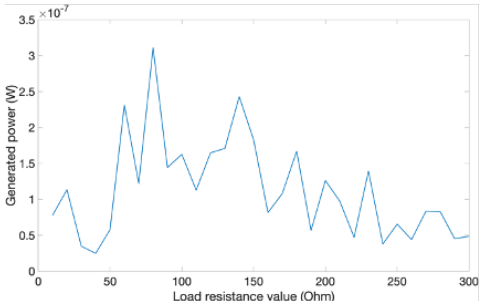

b) Water pump motor.

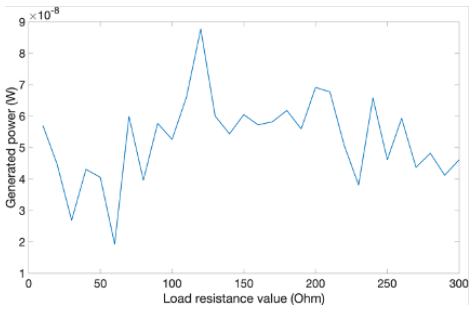

c) Car engine.

Figure 26-Power generated by each vibration source.

The results of power that the transducer can generate in each source of vibration vary for the source of lower leg walking between 0,4 uW and 1,7 uW, reaching its maximum with a load resistance of 275 ohm. When applied to the water pump motor, the transducer can generate between 0,025 uW and 0,33 uW, reaching its maximum power output with a load resistance at the transducer terminals of 80 ohm. When the car engine was simulated reached about 0,0088 uW at its maximum and a lowest value of 0,002 uW

VI. Conclusion

Energy can be harvested from a wide variety of sources and an alternative of the use of batteries to power the devices, it is the use of energy sources presented in environment like solar energy, thermal energy, wind energy, vibration energy, amongst others. Currently, it is increasingly necessary to recover all the energy possible, both ecologically and economically. Vibration is an example of an energy source that is rarely used, but with a great potential in the production of energy.

Vibration energy can be harvested mostly through piezoelectric, electrostatic, and electromagnetic transducers. Electromagnetic transducers harvest the vibration energy based on electromagnetic induction phenomenon. Levitation electromagnetic transducer type energy harvester was the chosen transducer topology to build and characterize because it avoids using the springs to make the magnets move, which brings the buckling effect to the transducer. Furthermore, it can be implemented in several situations and locals, and it does not require any specific vibration or movement.

To be possible to analyse and characterize the transducer, it was necessary to build a setup characterization capable to do it. This characterization setup consisted of two parts, the hardware part and the software part. The hardware part was composed by the instrumentation needed, and the software part was programmed in the LabVIEW software and its goal was to control the devices present in the hardware part and receive data from the system that would allow both the analysis and the characterization of the transducer ability to generate energy. Two separate programs were made in LabVIEW. One with the objective of optimising the results of the transducer, analysing at what distance the top magnets should be located and the position of the central magnets relative to the coil to achieve the maximum energy possible generated by the transducer. On the other hand, the second one with the objective of simulating several sources in the vibration generator, based on vibration data from real sources obtained data banks, and thus test the transducer on these real sources without leaving the laboratory. With these experiments, we can conclude that the initial aim of developing instrumentation to characterize the transducers and to emulate operational conditions when included on a IoT device was concluded with success.

The objective of illustrating the design and prototyping of an induction-based vibration energy transducer was also achieved however the transducer characteristics can be improved in the future.

REFERENCES

[1] R. Das *et al.*, "Enhanced room-temperature spin Seebeck effect in a YIG/C60/Pt layered heterostructure," *AIP Adv.*, vol. 8, no. 5, 2018, doi: 10.1063/1.5007233.

[2] Z. Chen, Y. Yang, Z. Lu, and Y. Luo, "Broadband characteristics of vibration energy harvesting using one-dimensional phononic piezoelectric cantilever beams," *Phys. B Condens. Matter*, vol. 410, no. 1, 2013, doi: 10.1016/j.physb.2012.10.029.

[3] W. Tian, Z. Ling, W. Yu, and J. Shi, "A review of MEMS scale piezoelectric energy harvester," *Applied Sciences (Switzerland)*, vol. 8, no. 4. 2018, doi: 10.3390/app8040645.

[4] [A. Mouapi, G. Vanessa Kamani, N. Hakem, and N. Kandil, "Multiphysics Simulation of Piezoelectric Cantilever Beam: Application in Automobile," *Mod. Environ. Sci. Eng.*, vol. 3, no. 01, 2017, doi: 10.15341/mese(2333-2581)/01.03.2017/005.

[5] S. W. Ibrahim and W. G. Ali, "A review on frequency tuning methods for piezoelectric energy harvesting systems," *Journal of Renewable and Sustainable Energy*, vol. 4, no. 6. 2012, doi: 10.1063/1.4766892.

[6] S. Boisseau, G. Despesse, and B. Ahmed, "Electrostatic Conversion for Vibration Energy Harvesting," in *Small-Scale Energy Harvesting*, 2012.

[7] Khan Academy, "What is Faraday's Law?," *Khan Academy*, 2020. .

[8] .Wei and X. Jing, "A comprehensive review on vibration energy harvesting: Modelling and realization," *Renewable and Sustainable Energy Reviews*, vol. 74. 2017, doi: 10.1016/j.rser.2017.01.073.

[9] M. C. Chiu, Y. C. Chang, L. J. Yeh, and C. H. Chung, "Numerical assessment of a one-mass spring-based electromagnetic energy harvester on a vibrating object," *Arch. Acoust.*, vol. 41, no. 1, 2016, doi: 10.1515/aoa-2016-0012.

[10] M. A. Halim, H. Cho, M. Salauddin, and J. Y. Park, "A miniaturized electromagnetic vibration energy harvester using flux-guided magnet stacks for human-body-induced motion," *Sensors Actuators, A Phys.*, vol. 249, 2016, doi: 10.1016/j.sna.2016.08.008.

[11] K. Kecik, A. Mitura, S. Lenci, and J. Warminski, "Energy harvesting from a magnetic levitation system," *Int. J. Non. Linear. Mech.*, vol. 94, 2017, doi: 10.1016/j.ijnonlinmec.2017.03.021.

[12] K. Kęcik, "Energy recovery from a non-linear electromagnetic system," *Acta Mech. Autom.*, vol. 12, no. 1, 2018, doi: 10.2478/ama-2018-0002.

.